Multistimuli-Responsive Self-Organized Liquid Crystal Bragg Gratings

Ran Chen, Yun-Han Lee, Tao Zhan, Kun Yin, Zhongwei An, and Shin-Tson Wu*

A simple approach is described to fabricate an electrically, thermally, and optically responsive polarization Bragg grating, using a dual-frequency liquid crystal (LC) doped with a photosensitive azobenzene chiral compound. Due to the employed dual-frequency LC, the Bragg reflection is switchable by an electric field. Based on the *trans-cis* isomerization of the azobenzene chiral dopant, the reflection wavelength of the LC Bragg gratings can be tuned across the visible wavelength by UV exposure. Meanwhile, the temperature responsivity of LC Bragg gratings is also characterized. Good agreement between experiment and theory is obtained. The circular polarization selectivity and external field tunability of LC Bragg gratings enrich these multifunctional devices and pave the way toward novel smart electro-optical devices.

Bragg gratings exhibit periodic index modulation which induces selective diffraction in wavelength and incident angle. It is widely applied for free-space/fiber optical filters,[1] wavelength multiplexers,[2] and waveguide couplers.[3] As a branch of high-efficiency Bragg gratings, reflective polarization volume grating (PVG) based on self-organized chiral nematic liquid crystal (LC) is a scientifically interesting and practically useful device.[4–6] Such a Bragg reflection based PVG exhibits several distinctive features: strong circular polarization selectivity, nearly 100% diffraction efficiency, and large deflection angle. Its potential applications include laser beam steering, waveguide coupler for augmented reality displays,[7] switches for telecommunication devices,[8] switchable add-drop filters, optical interconnects, dynamic equalizers, variable optical attenuators, and switchable filters.[9]

Dual-frequency liquid crystal (DFLC)[10–13] is a special class of mixture exhibiting a positive dielectric anisotropy ($\Delta\varepsilon > 0$) in the low frequency region (e.g., 1 kHz) and negative $\Delta\varepsilon$ as the frequency increases (e.g., 50 kHz) because of dielectric

R. Chen, Dr. Y.-H. Lee, T. Zhan, K. Yin, Prof. S.-T. Wu
Center for Research and Education in Optics and Lasers (CREOL)
The College of Optics and Photonics
University of Central Florida
Orlando, FL 32816, USA
E-mail: swu@creol.ucf.edu
R. Chen, Prof. Z. An
Key Laboratory of Applied Surface and Colloid Chemistry
School of Materials Science and Engineering
Shaanxi Normal University
Xi'an 710119, China

The ORCID identification number(s) for the author(s) of this article can be found under https://doi.org/10.1002/adom.201900101.

relaxation. The frequency where $\Delta\varepsilon = 0$ occurs is called crossover frequency (f_c). This property allows the reorientation of LC directors to be along or perpendicular to the electric field by simply switching the applied frequency. The PVG employing such a DFLC will respond to electrical stimulus. If we dope some chiral agents to the DFLC host, then the self-organized helical structure will be induced. Incorporating a photosensitive functional group such as azobenzene or azoxybenzene onto the chiral agent enables optical modulation of the helical twisting power (HTP) through UV or visible light illumination.[14,15] This kind of photoresponsivity has found interesting applications in all-optical devices and remote-control devices.[16,17] An LC diffraction grating with electrical- or photo-responsivity enables easy control of optical characteristics, which are highly desirable for designing useful optical devices.[18,19]

Previously,[20] LC diffraction gratings have been reported by employing nematic, smectic, cholesteric, and blue phase LCs. Although the switchability of LC gratings under external stimuli such as light, electric and magnetic fields, heat, and chemical composition have been proposed, these approaches mainly focus on the Raman–Nath transmissive LC gratings and their single or dual stimuli response behavior.

In this paper, we demonstrate a multistimuli-responsive reflective PVG based on a DFLC host doped with chiral agent and azobenzene. Such a device can respond to electrical, thermal, and optical stimuli. We investigate its electrical response to both low- and high-frequency signals, its photoresponse to UV light stimulation, and its thermal response to the operating temperature change.

Figure 1 illustrates the electric field responsivity of our PVG device. The helical axis orients following the periodic pattern on the bottom substrate and thereby forms the slanted planar texture. After applying a voltage (e.g., 50 V) at 1 kHz frequency, the LC directors are reoriented to homeotropic state and the Bragg reflection disappears. To switch from the homeotropic state back to the planar state, we can apply a high-frequency (50 kHz) voltage. Removing the voltage at this homeotropic state leads to the formation of a light-scattering focal conic texture. By switching the electric field from 1 to 50 kHz, the LC directors are realigned to the helical structure of the planar state. The corresponding transmission images from a polarized optical microscope are included in Figure 1. In the planar state, the asymmetric structure of PVG results in a small polarization
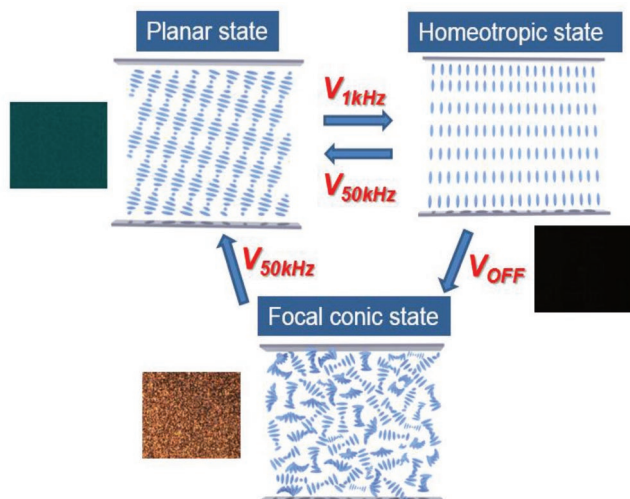
Figure 1. Schematic of the working principle of electrically switchable and tunable PVG device and corresponding micrographs in planar state, homeotropic state, and focal conic state.

rotation and the image appears greenish between crossed polarizers. As the voltage increases to 46 V, the LC directors are in homeotropic state and the image is black. Upon releasing voltage, the random reorientation of LC directors form focal conic state, resulting in light scattering. In the voltage-off state, the PVG reflects colors as **Figure 2**a depicts.

To study the electrical response of PVG, we prepared a sample with $d \approx 3$ µm. Upon applying a low-frequency (1 kHz) voltage, the planar structure of our sample progressively transforms to a focal conic state and finally homeotropic state.[21] As Figure 2b depicts, the transmittance at central wavelength (≈508 nm) changes from ≈3% to ≈100% as the voltage increases to 50 V, indicating the diffraction is switched off and the sample is in the homeotropic state. Interestingly, not only does the efficiency decrease with increasing voltage, but also the central wavelength shift toward blue region, indicating a reorientation of the helical axis. If we turn off the voltage at this transparent state, the relaxation from homeotropic state cannot return to the initial helical structure; instead, the focal conic structure appears. At a high frequency, MLC-2048 exhibits a negative $\Delta \varepsilon$, and thus the slanted planar structure is more stable in a voltage-on state. As Figure 2c depicts, at 50 kHz the focal conic state would be suppressed, and the cell could return to the planar state. As the high-frequency (50 kHz) voltage increases, diffraction efficiency increases to over 95%. From a careful comparison with Figure 2b, we find this restored planar state (by applying a high-frequency voltage) has a slightly broader bandwidth than the initial planar state. This indicates after driving at high voltage, the sample cannot fully return to the initial diffraction state. This is very different from previous work where dual-frequency cholesteric liquid crystal (CLC) was reported.[13] The discrepancy indicates the in-plane periodicity we introduced in the system altered the molecular relaxation process in a subtle way. Only through heating the sample to an
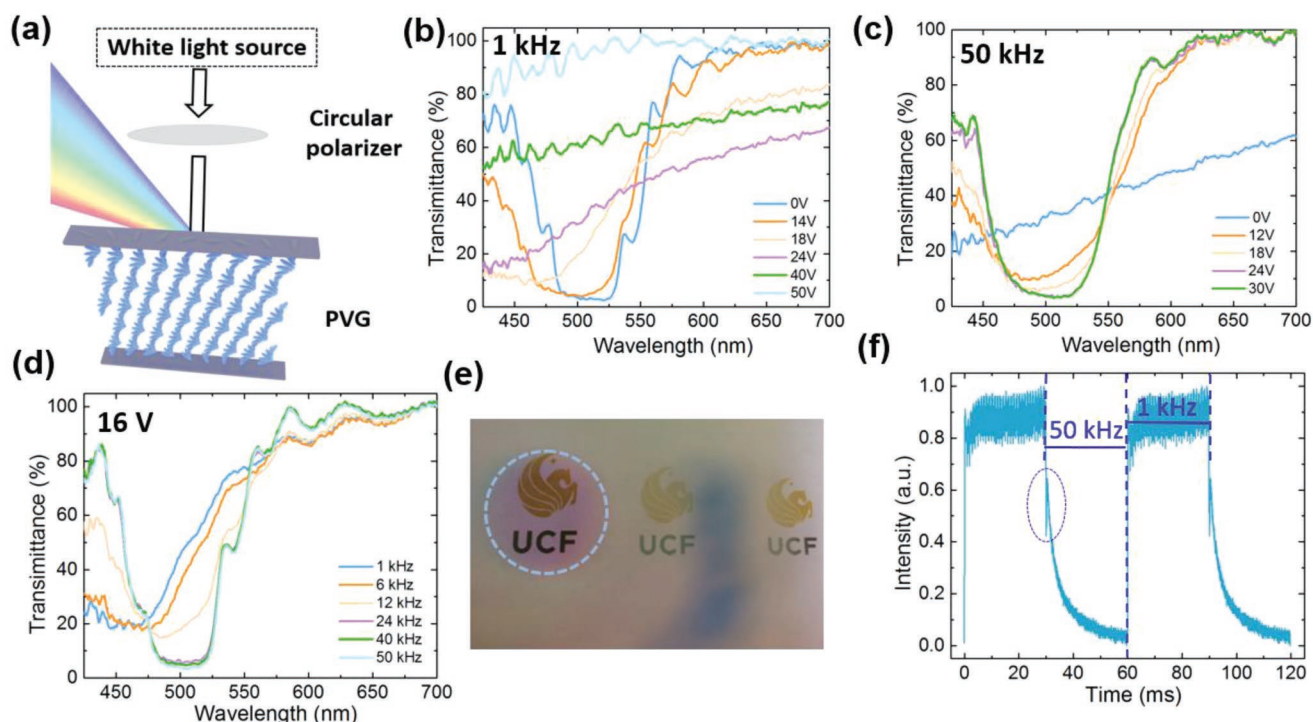

Figure 2. a) Schematic drawing of a reflective PVG under white light illumination. Electrically tuned transmission spectra of a PVG sample at various voltages: b) 1 kHz frequency and c) 50 kHz frequency. d) Frequency-dependent transmittance of a PVG cell at 16 V. The applied frequency ranges from 1 to 50 kHz. e) A photo taken through a PVG sample. The PVG region is circled in white dashed lines. The distance between PVG to camera was 1 cm, and the target was 10 cm away. f) Measured switching time of the PVG sample with d ≈ 3 µm. The backflow (circled region) increases the response time.

**ADVANCED
SCIENCE NEWS**
www.advancedsciencenews.com

**ADVANCED
OPTICAL
MATERIALS**
www.advopticalmat.de

isotropic state and then cooling it down to the room temperature, the initial grating structure can be recovered.[22] Interestingly, as shown in Figure 2d, it is found that if we apply a fixed voltage at an intermediate level (e.g., 16 V) and drive the sample with alternating frequency between 1 and 50 kHz (i.e., the sample did not go through a fully homeotropic state), heating was not required to promote the PVG sample back to its initial state (Figures S1 and S2, Supporting Information).

Response time is an important parameter for the LC devices.[23–25] By incorporating polymer network into an LC composite,[4,9] sub-millisecond response time has been demonstrated. However, such a polymer network is usually accompanied with hysteresis, light scattering, and high driving voltage. An alternative approach to reduce response time is through incorporating DFLCs. As shown in Figure 2e, the fabricated DFLC PVG sample is clear visually. The total (forward and backward) light scattering was measured to be ≈1% at λ = 633 nm with a standard integrating sphere. We measured the switching time between two voltage settings: (46 V, 1 kHz) and (30 V, 50 kHz). Note that the LC composite incorporated also azobenzene PSC-01, which will be stimulated by green through UV light. Therefore, the PVG sample was first exposed with UV light to move the central wavelength to 630 nm, and then a He–Ne laser (633 nm) was used as probing beam for measuring response time. The duration of each voltage setting was 30 ms. The response time is defined as transmittance change between 10% and 90%. As Figure 2f shows, the grating's turn-off time (from 50 to 1 kHz) was measured to be 1.36 ms, and turn-on time (from 1 to 50 kHz) was 11.55 ms. For a purely electrically

switchable PVG, it is possible to reduce the response time further by removing an azobenzene chiral dopant.

In our PVG, the turn-on process corresponds to the LC directors relaxing from homeotropic to planar state, as Figure 1 depicts. Such a turn-on process is accomplished by applying a high-frequency (50 kHz) voltage to bring the LC directors from homeotropic state back to initial planar state, because at 50 kHz the LC has a negative dielectric anisotropy ($\Delta\varepsilon < 0$). To erase the PVG, we applied a low-frequency voltage (1 kHz) to drive the LC directors from planar to homeotropic state. The response time of a DFLC device[10] is governed by the cell gap, viscoelastic constant, applied voltage, and threshold voltage at high frequency (50 kHz) and low frequency (1 kHz). However, in our PVG the ratio between turn-on time (11.55 ms) and turn-off time (1.36 ms) is about 1.37× larger than expected, as explained in the Supporting Information. This is because the backflow effect,[26] manifested as the optical bounce in Figure 2f, increases the turn-on time.

Chiral nematic liquid crystal is responsive to the temperature change,[27] but only few studies about the thermal response of LC gratings have been reported. For examples, Lin et al.[28] designed a thermally rotatable LC grating; Li and co-workers[29] demonstrated a thermoresponsive LC grating with reversible beam steering along orthogonal directions, and Sutherland et al.[30] reported that the central wavelength of LC Bragg grating exhibits a thermally induced blue shift. To investigate the thermal response of our PVG, we keep using the sample with $d \approx 3$ μm. We characterized its thermal behaviors by measuring the reflection spectra from 25 to 115 °C with a heating stage (Linkam, TMS94). **Figure 3**a depicts the recorded
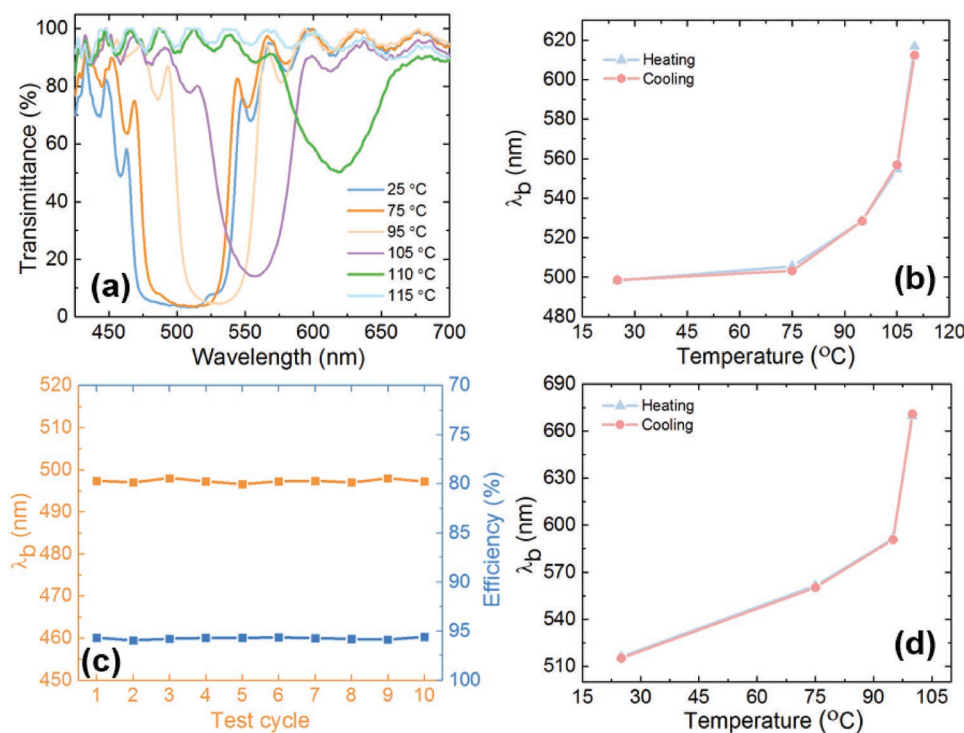

Figure 3. Wide-range spectrum scanning and repeatability in a PVG sample. a) Thermal tuning wavelength of a PVG upon heating; b,d) the corresponding Bragg wavelength λ_b with different temperature of our PVG and CLC samples during heating and cooling cycle; and c) the repeatability of a PVG sample.

ADVANCED
SCIENCE NEWS
www.advancedsciencenews.com

ADVANCED
OPTICAL
MATERIALS
www.advopticalmat.de

reflection notch from cyan (≈499 nm) to red (≈617 nm) upon heating. As the temperature increases, reflection band gradually shifts toward red but the diffraction efficiency declines. Above the clearing point, Bragg reflection vanishes. These phenomena originate from the combined effects of temperature dependent birefringence (Δn) and pitch length. The effect of temperature-dependent average refractive index ($<n>$) is negligible.[31,32] At first, the decrease of Δn leads to narrower bandwidth and decreased Bragg reflection as observed. As the temperature approaches clearing point, T_{NI} (110 °C), the bandwidth gets broadened and then vanished as the birefringence drops to zero (Figure S3, Supporting Information). This result originates from the decreased grating modulation (dΔn), which is also observed in other non-LC Bragg gratings.[33,34] The molecular interaction between azobenzene chiral dopant and liquid crystal host will also change with temperature.[35,36] In the case of R5011, this change in molecular force leads to a reduced helical twisting power on MLC-2048 at higher temperature, resulting in a rapid increase of pitch length[37] and the observed red shift (Figure 3a). During cooling, the PVG sample returns to its planar state and the Bragg reflection wavelength λ_b reaches its original position at 25 °C. Very little hysteresis is observed during this heating and cooling cycle (Figure 3b). That means such a thermal response is reversible. After ten heating–cooling cycles (25→115→25 °C), the reflection efficiency at λ_b and λ_b remain almost unchanged, which further confirms the repeatability of our PVG under thermal response (Figure 3c). The response time upon thermal annealing is dependent on the heating rate and the response speed of azobenzene and MLC-2048. Regardless of the heating rate, the Bragg reflection of this PVG device takes about 40 s to vanish.

To further understand the thermal response of our PVG (CLC with a specific pattern), we prepared a pure CLC sample (CLC with homogenous pattern). The Bragg reflection of our PVG vanishes at 115 °C, which is higher than the corresponding temperature of CLC sample. This implies a stronger molecular interaction in our PVG sample. Compared to our PVG, the larger redshift in λ_b of the CLC sample was observed with increasing temperature (Figure 3d), which further indicates that the pitch length increases with temperature in our case. In addition, the hysteresis between heating and cooling is insignificant for the pure CLC sample (Figure 3d), which presents that the molecular realignment of CLC sample at various temperature is easier to achieve.

All-optical control photonics is a fascinating subject. Pioneering work employing optical sensitive chiral dopants in liquid crystal hosts has demonstrated such possibility in liquid crystals for various applications, such as tunable lasers, gratings, and displays.[38,39] With intensive efforts,[40,41] it was found that incorporating azobenzene or azoxybenzene functional groups into chiral materials can maximize the optical sensitivity. In *trans*-form, the chiral molecules usually exhibit mesogenic phase and therefore have stronger molecular interaction with the LC host, resulting in a stronger helical twisting power (shorter pitch length). Typically, under violet or ultraviolet light illumination, they isomerize to *cis*-form, and therefore the helical power decreases, leading to a longer pitch length. The reversed process, *cis*-to-*trans* isomerization, can occur thermally or photochemically

with the irradiation of a visible light. With advanced molecular engineering, tuning range as wide as 2000 nm has been demonstrated,[42] while the response time is usually a few seconds to few minutes. Some reports indicated that the photoswitchable material doped distributed Bragg reflector (DBR) structures or photonic crystals showed a very little shifted wavelength,[43,44] a large reflective efficiency change[45,46] or very slow switching time[47] under photo-isomerization.

By incorporating the dynamic optical properties of an azo-LC mixture with the photonic properties of a PVG, we realized an optically tunable Bragg grating device. To explore such optical response, we used the same PVG sample with $d \approx 3$ μm. In the initial state, the PVG shows ≈98% Bragg reflection efficiency with a relatively wide bandwidth under circularly polarized light. The reflective diffraction efficiency of PVG was modulated by the exposure of 365 nm UV light at a very low power level (0.3 mW cm^{-2}). The Bragg wavelength red-shifted over time, as shown in **Figure 4**a. This is attributed to the decreased HTP of azobenzene chiral material from the *trans–cis* photoisomerization effect, which leads to a longer pitch length. The diffraction efficiency maintains over 96% in almost the entire visible spectral region. Figure 4b,c shows the dependence of Bragg reflection band λ_b and bandwidth (full-width at half-maximum) $\Delta \lambda$ on the UV exposure time. A relatively large redshift (about 135 nm) in λ_b was observed with increasing UV exposure time. After ≈3 min of UV exposure, the bandwidth $\Delta \lambda$ increases from 96.7 to 123.2 nm. Upon further exposure to UV light, both λ_b and $\Delta \lambda$ gradually saturate.

Although λ_b undergoes a relatively large blueshift (about 100 nm) by increasing the visible light exposure time ($\lambda = 532$ nm at 0.5 mW cm^{-2}), this system could not switch back to its original state by visible light illumination (Figure S4, Supporting Information). This is attributed to the irreversibility on HTP change of our azobenzene chiral dopant under light irradiation.[48] By heating the sample to an isotropic state and then cooling it down to the room temperature, the slanted planar structure can be fully recovered. After detailed formula derivation (Figure S5, Supporting Information), the solid lines in Figure 4b,c represent fittings with following equations (assume Bragg angle remains at a constant Φ).[49]

$$\lambda_b = \frac{\langle n \rangle \cos \Phi}{C_{t0} e^{-t/\tau} (\beta_{trans} - \beta_{cis}) + C_{t0} \beta_{cis} + C_0 \beta_0} \quad (1)$$

$$\Delta \lambda = \frac{\Delta n \cos \Phi}{C_{t0} e^{-t/\tau} (\beta_{trans} - \beta_{cis}) + C_{t0} \beta_{cis} + C_0 \beta_0} \quad (2)$$

In Equation (1) and Equation (2), C_{t0} and C_0 represent the concentration of *trans*-azobenzene and R5011 at $t = 0$, respectively, and τ is the isomerization time constant. Let us assume the HTP of *trans*-azobenzene PSC-01, *cis*-azobenzene PSC-01 and R5011 is β_{trans}, β_{cis} and β_0, and the $<n>$ and Δn are the average refractive index and birefringence of this employed LC mixture, then Equations (1) and (2) can be simplified as

$$\lambda_b = A_1 / \left(e^{-t/\tau} + B \right) \quad (3)$$

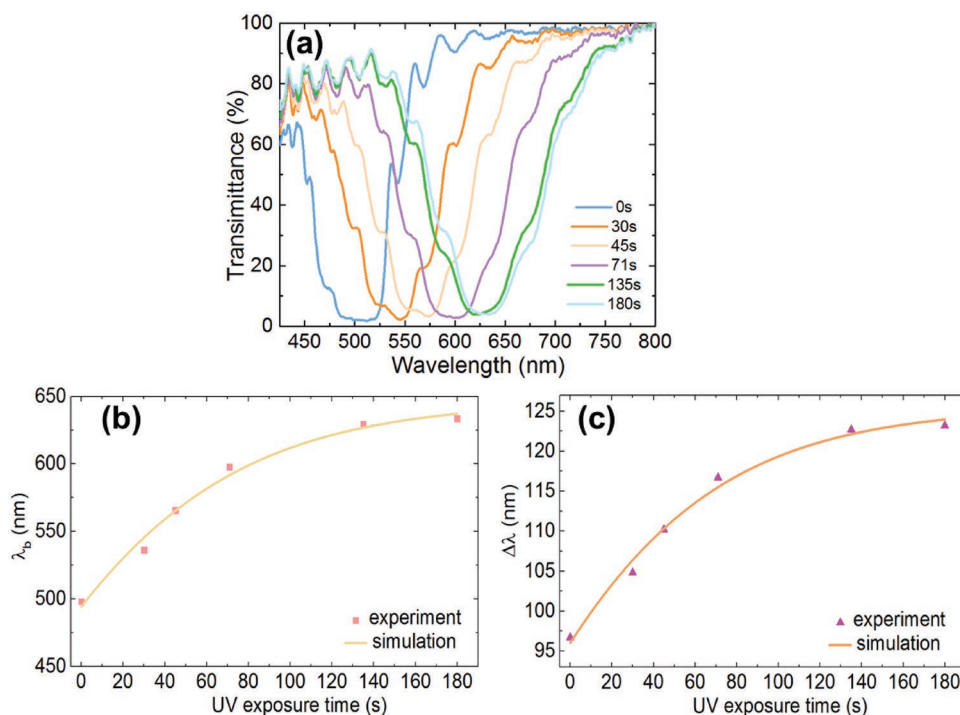$$\Delta \lambda = A_2 / \left(e^{-t/\tau} + B \right) \quad (4)$$

**ADVANCED
SCIENCE NEWS**
www.advancedsciencenews.com

**ADVANCED
OPTICAL
MATERIALS**
www.advopticalmat.de

Figure 4. a) Spectra of PVG at different UV exposure time ($\lambda = 365$ nm, 0.3 mW cm^{-2}) and b,c) the corresponding Bragg wavelength λ_b and bandwidth $\Delta\lambda$ with different UV exposure time. Dots are experimental data and solid lines are fitting curves with Equation (1) and Equation (2).

Through fittings, we find $A_1 = 2102.17$ µm, $A_2 = 409.33$ µm, $B = 3.25$, and $\tau = 59$s. Therefore, we can establish a correlation between exposure time and central wavelength and bandwidth of the photoresponsive PVG.

In conclusion, a novel multistimuli-responsive LC Bragg grating was demonstrated with a DFLC host doped with a photosensitive chiral compound. The electrical, thermal, and photoresponsivities of the device were investigated. For electrical control, the switching time of our PVG is around 10 milliseconds. The optical performance allows for modulation of Bragg wavelength over the entire visible spectrum. A correlation between exposure time, central wavelength, and bandwidth of the photoresponsive PVG was established. Meanwhile, the thermal response shows large redshift and it is relatively insensitive to the temperature fluctuation at room temperature. These unique properties of responsive Bragg gratings offer potential applications for active electrical/optical control of waveguide-coupling gratings or beam steering devices.

Experimental Section

Material Preparation: The employed DFLC host was MLC-2048 (Merck), whose physical properties are listed as follows: clearing point (T_{NI}) = 108.5 °C, $\Delta\varepsilon = 2.5$ at 1 kHz and -1.2 at 50 kHz,[50] crossover frequency $f_c = 12$ kHz, and refractive indices $n_e = 1.71$, $n_o = 1.50$ at $\lambda = 633$ nm and 23 °C. The chiral dopant was R5011 (HCCH, helical twisting power HTP ≈ 110 µm^{-1}) and the azobenzene chiral dopant PSC-01 (HTP ≈ 64 µm^{-1}) was from PKU, whose molecular structure is shown in Lee et al.[49] The weight ratios of MLC-2048, R5011, and PSC-01 were 95.9:2.0:2.1.

Sample Fabrication: One clean indium tin oxide (ITO) glass substrate was treated with UV-ozone (30 min, Ossila) and then spin-coated with

a photo-alignment material (Brilliant yellow, at 2000 rpm for 30 s) to create a uniform thin film on the substrate. This substrate was then exposed to the interference patterns using a He–Cd laser (Kimmon, $\lambda = 457$ nm). Detailed interference exposure process has been described in Lee et al.[3] In summary, the two opposite-handed circularly polarized beams were aligned to make an angle $\alpha = 40°$ onto the coated substrate to generate a periodicity $\Lambda x \approx 650$ nm. The other clean ITO substrate was spin-coated with polyimide at 500 rpm for 7 s and 1500 rpm for 30 s, and prebaked at 95 °C for 5 min and then baked at 180 °C for 60 min. Note that this substrate had no rubbing treatment. Then, these two ITO substrates were sealed to form a cell (the average cell gap is $d = 3$ µm controlled by silica spacers). The LC mixture was infiltrated into the cell at 120 °C and the cell was cooled down slowly to the room temperature (23 °C). The pure CLC sample was prepared with the same LC mixture in a commercial homogenous cell, whose cell gap was $d = 3.3$ µm.

Optical Measurements: To characterize the PVG, a white light source (Mikropack DH-2000) and an optical fiber spectrometer (Ocean Optics HR2000CG-UV-NIR) were used to measure the reflection spectra. To measure the diffraction efficiency, the sample was placed on a spectrometer with circularly polarized light at normal incidence. Various frequency-modulated square-wave voltages were supplied from an arbitrary function generator (Agilent 33120A) and high voltage linear amplifier (FLC Electronics A400D) to switch the states and to induce color changes. The dynamic switching time was measured with an oscilloscope (Tektronix TDS3032B); the experimental measurement is described in Figure S6 in the Supporting Information. A He–Ne laser ($\lambda = 632.8$ nm) served as the light source, a LabVIEW data acquisition system controlled the low- and high-frequency signals, and an oscilloscope recorded the switching time.

Supporting Information

Supporting Information is available from the Wiley Online Library or from the author.

Acknowledgements

Conflict of Interest

The authors declare no conflict of interest.

Keywords

[1] W. Zhang, J. Yao, *Nat. Commun.* **2018**, *9*, 1396.
[2] C. A. Brackett, *IEEE J. Sel. Areas Commun.* **1990**, *8*, 948.
[3] Y. H. Lee, K. Yin, S. T. Wu, *Opt. Express* **2017**, *25*, 27008.
[4] J. Kobashi, H. Yoshida, M. Ozaki, *Nat. Photonics* **2016**, *10*, 389.
[5] Y. Weng, D. Xu, Y. Zhang, X. Li, S.-T. Wu, *Opt. Express* **2016**, *24*, 17746.
[6] J. Kobashi, Y. Mohri, H. Yoshida, M. Ozaki, *Opt. Data Process. Storage* **2017**, *3*, 61.
[7] V. Vinvogradova, A. Khizhnyaka, L. Kutulyaa, Y. Reznikova, V. Resihetnyaka, *Mol. Cryst. Liq. Cryst.* **1990**, *192*, 273.
[8] S. Yeralan, J. Gunther, D. L. Ritums, R. Cid, M. M. Popovich, *Opt. Eng.* **2002**, *41*, 1774.
[9] G. P. Crawford, *Opt. Photonics News* **2003**, *14*, 54.
[10] H. Xianyu, S.-T. Wu, C.-L. Lin, *Liq. Cryst.* **2009**, *36*, 717.
[11] M. Schadt, *Mol. Cryst. Liq. Cryst.* **1982**, *89*, 77.
[12] M. Xu, D. K. Yang, *Jpn. J. Appl. Phys.* **1999**, *38*, 6827.
[13] Y.-C. Hsiao, C.-Y. Tang, W. Lee, *Opt. Express* **2011**, *19*, 9744.
[14] B. L. Feringa, W. F. Jager, B. de Lange, E. W. Meijer, *J. Am. Chem. Soc.* **1991**, *113*, 5468.
[15] L. Wang, H. Dong, Y. Li, C. Xue, L.-D. Sun, C.-H. Yan, Q. Li, *J. Am. Chem. Soc.* **2014**, *136*, 4480.
[16] H.-C. Jau, P.-C. Chou, C.-W. Chen, C.-C. Li, S.-E. Leng, C.-H. Lee, T.-H. Lin, *Opt. Express* **2018**, *26*, 781.
[17] Y.-C. Liu, K.-T. Cheng, Y.-D. Chen, A. Y.-G. Fuh, *Opt. Express* **2013**, *21*, 18492.
[18] A. Ryabchun, A. Bobrovsky, *Adv. Opt. Mater.* **2018**, *6*, 1800335.
[19] H. K. Bisoyi, T. J. Bunning, Q. Li, *Adv. Mater.* **2018**, *30*, 1706512.
[20] R. S. Zola, H. K. Bisoyi, H. Wang, A. M. Urbas, T. J. Bunning, Q. Li, *Adv. Mater.* **2018**, *30*, 1806172.
[21] E. Oton, E. Netter, *Opt. Express* **2017**, *25*, 13314.
[22] D. J. Davies, A. R. Vaccaro, S. M. Morris, N. Herzer, A. P. Schenning, C. W. Bastiaansen, *Adv. Funct. Mater.* **2013**, *23*, 2723.
[23] Y. H. Lee, F. Peng, S. T. Wu, *Opt. Express* **2016**, *24*, 1668.
[24] T. J. Bunning, L. V. Natarajan, V. P. Tondiglia, R. L. Sutherland, *Annu. Rev. Mater. Sci.* **2000**, *30*, 83.
[25] A. Urbas, V. Tondiglia, L. Natarajan, R. Sutherland, H. Yu, J. H. Li, T. Bunning, *J. Am. Chem. Soc.* **2004**, *126*, 13580.
[26] H. Wang, T. X. Wu, S. Gauza, J. R. Wu, S. T. Wu, *Liq. Cryst.* **2006**, *33*, 91.
[27] M. E. McConney, V. P. Tondiglia, J. M. Hurtubise, L. V. Natarajan, T. J. White, T. J. Bunning, *Adv. Mater.* **2011**, *23*, 1453.
[28] C. H. Lin, R. H. Chiang, S. H. Liu, C. T. Kuo, C. Y. Huang, *Opt. Express* **2012**, *20*, 26837.
[29] L. Zhang, L. Wang, U. S. Hiremath, H. K. Bisoyi, G. G. Nair, C. V. Yelamaggad, A. M. Urbas, T. J. Bunning, Q. Li, *Adv. Mater.* **2017**, *29*, 1700676.
[30] R. L. Sutherland, V. P. Tondiglia, L. V. Natarajan, J. M. Wofford, S. A. Siwecki, G. Cook, D. R. Evans, P. F. Lloyd, T. J. Bunning, *Proc. SPIE* **2007**, *6487*, 64870V.
[31] P. Lova, G. Manfredi, D. Comoretto, *Adv. Opt. Mater.* **2018**, *6*, 1800730.
[32] S. N. Kasarova, N. G. Sultanova, I. D. Nikolov, *J. Phys.: Conf. Ser.* **2010**, *253*, 012028.
[33] O. M. Efimov, L. B. Glebov, L. N. Glebova, K. C. Richardson, V. I. Smirnov, *Appl. Opt.* **1999**, *38*, 619.
[34] L. B. Glebov, *Glass Sci. Technol.* **2002**, *75*, 73.
[35] D. Y. Kim, S. A. Lee, M. Park, Y. J. Choi, S. W. Kang, K. U. Jeong, *Soft Matter* **2015**, *11*, 2924.
[36] M. Mathews, R. S. Zola, D. K. Yang, Q. Li, *J. Mater. Chem.* **2011**, *21*, 2098.
[37] T. J. White, M. E. McConney, T. J. Bunning, *J. Mater. Chem.* **2010**, *20*, 9832.
[38] Z. G. Zheng, Y. Li, H. K. Bisoyi, L. Wang, T. J. Bunning, Q. Li, *Nature* **2016**, *531*, 352.
[39] A. Urbas, J. Klosterman, V. Tondiglia, L. Natarajan, R. Sutherland, O. Tsutsumi, T. Ikeda, T. Bunning, *Adv. Mater.* **2004**, *16*, 1453.
[40] U. A. Hrozhyk, S. V. Serak, N. V. Tabiryan, T. J. Bunning, *Adv. Funct. Mater.* **2007**, *17*, 1735.
[41] L. De Sio, L. Ricciardi, S. Serak, M. La Deda, N. Tabiryan, C. Umeton, *J. Mater. Chem.* **2012**, *22*, 6669.
[42] T. J. White, R. L. Bricker, L. V. Natarajan, N. V. Tabiryan, L. Green, Q. Li, T. J. Bunning, *Adv. Funct. Mater.* **2009**, *19*, 3484.
[43] R. Piron, E. Toussaere, D. Josse, J. Zyss, *Appl. Phys. Lett.* **2000**, *77*, 2461.
[44] R. J. Knarr III, G. Manfredi, E. Martinelli, M. Pannocchia, D. Repetto, C. Mennucci, I. Solano, M. Canepa, F. B. de Mongeot, G. Galli, D. Comoretto, *Polymer* **2016**, *84*, 383.
[45] R. Yagi, H. Katae, Y. Kuwahara, S. N. Kim, T. Ogata, S. Kurihara, *Polymer* **2014**, *55*, 1120.
[46] M. Moritsugu, T. Ishikawa, T. Kawata, T. Ogata, Y. Kuwahara, S. Kurihara, *Macromol. Rapid Commun.* **2011**, *32*, 1546.
[47] M. Kamenjicki Maurer, I. K. Lednev, S. A. Asher, *Adv. Funct. Mater.* **2005**, *15*, 1401.
[48] C. C. Li, C. W. Chen, C. K. Yu, H. C. Jau, J. A. Lv, X. Qing, C. F. Lin, C. Y. Cheng, C. Y. Wang, J. Wei, Y. Yu, *Adv. Opt. Mater.* **2017**, *5*, 1600824.
[49] Y. H. Lee, L. Wang, H. Yang, S. T. Wu, *Opt. Express* **2015**, *23*, 22658.
[50] A. B. Golovin, S. V. Shiyanovskii, O. D. Lavrentovich, *Proc. SPIE* **2005**, *5741*, 146.